Interferon Type I Regulates Inflammasome Activation and High Mobility Group Box 1 Translocation in Hepatocytes During *Ehrlichia*-Induced Acute Liver Injury

Muhamuda Kader,[1*] Abdeljabar El Andaloussi,[2*] Jennie Vorhaour ,[1] Kenichi Tamama,[1] Natalia Nieto ,[2] Melanie J. Scott,[3] and Nahed Ismail[2]

Inflammasomes are an important innate immune host defense against intracellular microbial infection. Activation of inflammasomes by microbial or host ligands results in cleavage of caspase-1 (canonical pathway) or caspase-11 (non-canonical pathway), release of interleukin (IL)-1β, IL-18, high mobility group box 1 (HMGB1), and inflammatory cell death known as pyroptosis. *Ehrlichia* are obligate, intracellular, gram-negative bacteria that lack lipopolysaccharide but cause potentially life-threatening monocytic ehrlichiosis in humans and mice that is characterized by liver injury followed by sepsis and multiorgan failure. Employing murine models of mild and fatal ehrlichiosis caused by infection with mildly and highly virulent *Ehrlichia muris* (EM) and *Ixodes ovatus Ehrlichia* (IOE), respectively, we have previously shown that IOE infection triggers type I interferon (IFN-I) response and deleterious caspase-11 activation in liver tissues, which promotes liver injury and sepsis. In this study, we examined the contribution of IFN-I signaling in hepatocytes (HCs) to *Ehrlichia*-induced liver injury. Compared to EM infection, we found that IOE enter and replicate *in vitro* cultured primary murine HCs and induce secretion of IFNβ and several chemokines, including regulated upon activation, normal T-cell expressed, and secreted (RANTES), monocyte chemoattractant protein 1 (MCP1), monokine induced by gamma (MIG)/chemokine (C-X-C motif) ligand 9 (CXCL9), macrophage inflammatory protein 1 alpha (MIP1α), keratinocyte-derived chemokine (KC), and granulocyte-macrophage colony-stimulating factor (GM-CSF). Notably, *in vitro* stimulation of uninfected and *Ehrlichia*-infected HCs with recombinant IFNβ triggered activation of caspase-1/11, cytosolic translocation of HMGB1, and enhanced autophagy and intracellular bacterial replication. Secretion of HMGB1 by IOE-infected HCs was dependent on caspase-11. Primary HCs from IOE- but not EM-infected mice also expressed active caspase-1/11. *Conclusion:* HC-specific IFN-I signaling may exacerbate liver pathology during infection with obligate intracellular *Ehrlichia* by promoting bacterial replication and detrimental caspase-11-mediated inflammasome activation. (*Hepatology Communications* 2021;5:33-51).

Inflammasomes are cytosolic protein complexes that sense intracellular pathogen-associated molecular patterns (PAMPs) and damage-associated molecular patterns (DAMPs).[1,2] Nucleotide-binding oligomerization domain-like receptor family pyrin domain containing 3 (NLRP3) is a major inflammasome

Abbreviations: ATG12, autophagy-related 12; CCL, chemokine (C-C motif) ligand; CXCL, chemokine (C-X-C motif) ligand; DAMP, damage-associated molecular pattern; DAPI, 4′,6-diamidino-2-phenylindole; dsb, disulfide bond formation protein gene; ELISA, enzyme-linked immunosorbent assay; EM, Ehrlichia muris; GAPDH, glyceraldehyde 3-phosphate dehydrogenase; GM-CSF, granulocyte-macrophage colony-stimulating factor; HC, hepatocyte; HMGB1, high mobility group box 1; IFNAR, type I interferon receptor; IFN-I, type I interferon; IL, interleukin; IOE, Ixodes ovatus Ehrlichia; IRF, interferon regulatory factor; KC, keratinocyte-derived chemokine; LC3, Microtubule-associated protein 1A/1B, light-chain 3; LDH, lactate dehydrogenase; LPS, lipopolysaccharide; MAPK, mitogen-activated protein kinase; MCP1, monocyte chemoattractant protein 1; MIG, monokine induced by gamma; MIP1α, macrophage inflammatory protein 1 alpha; MOI, multiplicity of infection; mRNA, messenger RNA; mt, mitochondrial; mTORC1, mammalian target of rapamycin complex 1; MyD88, myeloid differentiation primary response 88; NLRP3, nucleotide-binding oligomerization domain-like receptor family pyrin domain containing 3; p62/SQSTM1, sequestosome 1; PAMP, pathogen-associated molecular pattern; pS6, phosphorylated S6 protein; qPCR, quantitative real-time polymerase chain reaction; qRT-PCR, quantitative reverse-transcription polymerase chain reaction; RANTES, regulated upon activation, normal T-cell expressed, and secreted; rDNA, ribosomal DNA; rIFN, recombinant interferon; S6, protein S6; TRP, tandem repeat protein; WT, wild type.

complex that consists of NLRP3, apoptosis-associated speck-like protein with caspase activation and recruitment domain (ASC), and (pro)-caspase-1.[3,4] Activation of NLRP3 by PAMPs or DAMPs induces cleavage/activation of caspase-1 followed by cleavage of pro-interleukin (pro-IL)-1β and pro-IL-18 into biologically active IL-1β and IL-18 cytokines. This pathway is referred to as the canonical inflammasome pathway.[4] Recently, a noncanonical inflammasome pathway has been described and is mediated by caspase-11 activation following sensing of cytosolic lipopolysaccharide (LPS).[5] Active caspase-11 enhances the activation of caspase-1 and the subsequent secretion of IL-1β, IL-1α, and high mobility group box 1 (HMGB1) as well as induction of inflammatory cell death known as pyroptosis.[6] Although the NLRP3 inflammasome plays protective roles in certain infection models by promoting pathogen elimination, NLRP3 can also play a deleterious role in host responses to certain microbial infections through excessive inflammation and cell death.[7,8]

Ehrlichia are obligate intracellular gram-negative bacterial pathogens that cause potentially fatal human monocytic ehrlichiosis (HME).[9] If not treated early in infection, patients develop complications, such as sepsis with multiorgan failure.[10,11] Unlike other gram-negative bacteria, *Ehrlichia* lacks peptidoglycan and LPS.[12,13] The liver is the main site of infection and pathology during the early stage of ehrlichiosis. We have shown that virulent *Ixodes ovatus Ehrlichia* (IOE) triggers NLRP3 inflammasome activation in the liver, which leads to extensive and dysregulated adaptive immune responses, inflammation, and liver immunopathology.[10,14,15] We recently showed that canonical and noncanonical inflammasome activation in IOE-infected macrophages is due to inhibition of autophagy induction by myeloid differentiation primary response 88 (MyD88)-dependent mammalian target of rapamycin complex 1 (mTORC1) activation.[10] Interestingly, we and others have demonstrated that *Ehrlichia* sequesters autophagy proteins as nutrients to further support their own survival and replication.[10,16-18] Thus, while suppressed autophagy by MyD88 restricts bacterial replication by inhibiting autophagy, it enhances inflammasome activation during fatal *Ehrlichia* infection.

Recently, we and other investigators have demonstrated that type I interferon (IFN-I) receptor (IFNAR) signaling is the master regulator of *Ehrlichia*-induced liver injury and sepsis.[10,14,19] However, the exact cellular source of IFNAR-mediated inflammasome activation during virulent *Ehrlichia* infection

Received February 12, 2020; accepted August 27, 2020.

Additional Supporting Information may be found at onlinelibrary.wiley.com/doi/10.1002/hep4.1608/suppinfo.

Supported by the National Institutes of Health, National Institute of General Medical Sciences (Grants R56 AI097679 to N.I.; Grants RO1 HL141080 and RO1 GM102146 To M.J.S.; Grants RO1 AA025907 and RO1 DK111677 to N.N.).

**These authors contributed equally to this work.*

View this article online at wileyonlinelibrary.com.

DOI 10.1002/hep4.1608

Potential conflict of interest: Dr. Nieto consults for Ionis Pharmaceuticals. The other authors have nothing to report.

ARTICLE INFORMATION:

From the [1]Department of Pathology, School of Medicine, University of Pittsburgh, Pittsburgh, PA, USA; [2]Department of Pathology, College of Medicine, University of Illinois at Chicago, Chicago, IL, USA; [3]Department of Surgery, School of Medicine, University of Pittsburgh, Pittsburgh, PA, USA.

ADDRESS CORRESPONDENCE AND REPRINT REQUESTS TO:

Nahed Ismail, M.D., Ph.D.
Department of Pathology, University of Illinois at Chicago
840 South Wood Street, 260F, (MC 847)
Chicago, IL, 60612, USA
E-mail: ismail7@uic.edu
Tel.: +1-312-355-0092

TABLE 1. PRIMER SEQUENCES FROM INTEGRATED DNA TECHNOLOGIES

Primer Name	Forward 5′-3′	Reverse 5′-3′
DSB	CAG GAT GGT AAA GTA CGT GTG A	TAG CTA ACG CTG CCT GAA CA
16S rDNA	AGC AAT GCC TCC TGC ACC ACC AAC	CCA CAT CAC CCC TCT ACC TC
HMGB1	GGCGAGCATCCTGGCTTATC	GGCTGCTTGTCATCTGCTG
IL-1β	ACC CTG CAG TGG TTC GAG	TTG CAC AAG GAA GCT TGG
Caspase-1	ATC ATT TCC GCG GTT GAA T	AAT TGC TGT GTG CGC ATG T
Caspase-11	ACA ATG CTG AAC GCA GTG AC	CTG GTT CCT CCA TTT CCA GA
ATG12	GCTACAGCACTACTTGGGTCA	GACCTCAAAAACTCGTTCACAGA
IFNAR	GGA TGG CAG TGA CAG TGAC	ATG GAG AAC CCT CAG AAA CAC
IFNβ	AGG CAG TGG GAA CAA GAC AG	AAA CTT CCT GAC GCC ACC C
IRF7	GCGTACCCTGGAAGCATTTC	GCACAGCGGAAGTTGGTCT
GAPDH	CAA CTA CAT GGT CTA CAT GTT C	TCG CTC CTG GAA GAT G

remains elusive. *Ehrlichia* infect leukocytes, endothelial cells, and hepatocytes (HCs) in mice and humans. Studies have suggested that HCs are not simply target cells for infectious pathogens but can also regulate inflammation during infection through innate and adaptive immunity.[20,21] However, little is known about the contribution of HCs to the pathogenesis of *Ehrlichia*-induced liver injury and sepsis.

In this study, we examined the regulation of the inflammasomes and of autophagy by paracrine IFNAR signaling in HCs following infection with virulent IOE. Our data show that IFNAR signaling in HCs promotes the development of inflammation and enhances bacterial replication through mechanisms that involve inflammasome activation, HMGB1 cytosolic translocation, and induction of autophagy.

Materials and Methods

MICE AND *EHRLICHIA* SPECIES

Female, 6-8-week-old, C57BL/6 wild-type (WT) mice were obtained from Jackson Laboratory (Bar Harbor, ME). These mice were used to isolate primary HCs. All mice were maintained in a specific pathogen-free environment at the University of Pittsburgh Animal Care Facility. Two *Ehrlichia* species were used in this study: a highly virulent IOE and mildly virulent *Ehrlichia muris* (EM). These strains were provided by Dr. Yasuko Rikihisa (Ohio State University, Columbus, OH). IOE and EM cause fatal and mild ehrlichiosis in C57BL/6 mice, respectively.[18]

ISOLATION OF PRIMARY MURINE HCs

Primary HCs were isolated using a two-step perfusion method as described.[22] Isolated HCs were seeded on collagen-coated culture dishes and used for experiments on the following day.

IN VITRO EHRLICHIA INFECTION

IOE and EM organisms were added to the HC cultures at a multiplicity of infection (MOI) of 5. Uninfected or infected cells were cultured in the absence or presence of recombinant IFNβ (rIFNβ; 500 IU/mL) and a caspase-1 inhibitor (10 μm/mL) (Enzo Life Sciences, Ann Arbor, MI). All cells were collected at 24 hours postinfection for further analysis by western blot. The cell-culture media was collected and stored at −80°C for cytokine analysis.

BACTERIAL BURDEN MEASUREMENT USING QUANTITATIVE REAL-TIME PCR

The number of intracellular *Ehrlichia* (IOE or EM) in infected HCs was determined at 24 hours and 48 hours postinfection by quantitative real-time polymerase chain reaction (qPCR) amplifying the conserved *Ehrlichia* disulfide bond formation protein (*dsb*) gene as described.[23] The primers used for *Ehrlichia dsb* are listed in Table 1. The relative copy number of intracellular *Ehrlichia* harvested from *in vitro*-infected cells was determined by normalization of the *Ehrlichia* copy number to glyceraldehyde 3-phosphate dehydrogenase (GAPDH). In some

experiments, the number of live replicating bacteria was determined by quantitative reverse-transcription PCR (qRT-PCR) analysis of the 16S ribosomal DNA (rDNA) as described.[23] PCR primer sets are listed in Table 1. The *GAPDH* gene was amplified for normalization of the complementary DNA (cDNA) amount used in qRT-PCR. Reactions were performed in triplicate, and the data were analyzed using the $2^{-\Delta\Delta Ct}$ method as described.[24]

MEASUREMENT OF CYTOKINES AND CHEMOKINES BY ENZYME-LINKED IMMUNOSORBENT ASSAY

Levels of proinflammatory cytokines and chemokines were measured by multiplex enzyme-linked immunosorbent assay (ELISA) (Bio-Plex Pro TM Mouse Cytokine 23 plex #MD60009RDPD; Biorad, Hercules, CA) following the manufacturer's recommendation. The concentration of HMGB1 was determined using the mouse HMGB1 ELISA Kit (LifeSpan Bioscience, Seattle, WI). The concentration of IL-1α, IL-1β, and IFNβ was measured with a commercial ELISA kit (R&D Systems, Minneapolis, MN).

WESTERN BLOT

HCs were lysed in radio immunoprecipitation assay buffer (Thermo Fisher Scientific, Waltham, MA) supplemented with protease inhibitors and 1 mM phenyl methyl sulphonyl fluoride. Membranes were processed and probed with the following antibodies according to standard protocols: anti-caspase-1 (1:100) (EMD Millipore, Billerica, MA), anti-caspase-11 (1:100), and anti-LC3AB (Sigma-Aldrich, St. Louis, MO). Antibodies against sequestosome 1 (p62/SQSTM1), protein S6 (S6), and phosphorylated S6 (pS6) were from Cell Signaling Inc. Blots were stripped and reprobed with anti-GAPDH (1:5,000) (Sigma-Aldrich) or anti-beta actin (1:2,500) (Abcam, Cambridge, MA) as loading controls. The density of bands in western blots was determined using ImageJ software version 1.48 (National Institutes of Health [NIH], Bethesda, MD). The ratio of LC3II:LC3I was determined by normalization of LC3II and LC3I to GAPDH.

IMMUNOFLUORESCENCE STAINING AND CONFOCAL MICROSCOPY

Staining of LC3 puncta, LysoTracker staining of acidified lysosomes, *Ehrlichia*, and HMGB1 aggregates as well as quantification by confocal microscopy were performed as described.[7,8]

Additional information on the Confocal Staining protocols are being provided in the Supplementary Methods Section.

IMAGE ANALYSIS

Analysis of HMGB1 and LC3B puncta as well as colocalization of LC3B with LysoTracker were performed using the NIH ImageJ software package. We analyzed 40-50 cells per group from three independent experiments. The colocalization images were analyzed using PCI software by counting the number of yellow aggregates per cell. Results were presented as average HMGB1 or LC3 puncta per cell or the number of colocalized LC3 puncta with lysosome per cell. At least 10 fields of view for each sample were quantified for each experimental group across at least three independent experiments. Data were analyzed as average ± SD.

STATISTICAL ANALYSIS

All data presented are representative of at least three independent experiments that yielded similar results. The two-tailed *t* test was used for comparison of mean values for two experimental groups, and a one-way analysis of variance was used for comparisons of multiple experimental groups. Data are expressed as means ± SD.

Results

EHRLICHIA INVADE AND REPLICATE INTRACELLULARLY IN HCs

Our previous studies have shown that intraperitoneal infection with IOE causes acute fatal toxic shock-like syndrome, characterized by extensive foci of hepatic apoptosis and necrosis followed by multiorgan

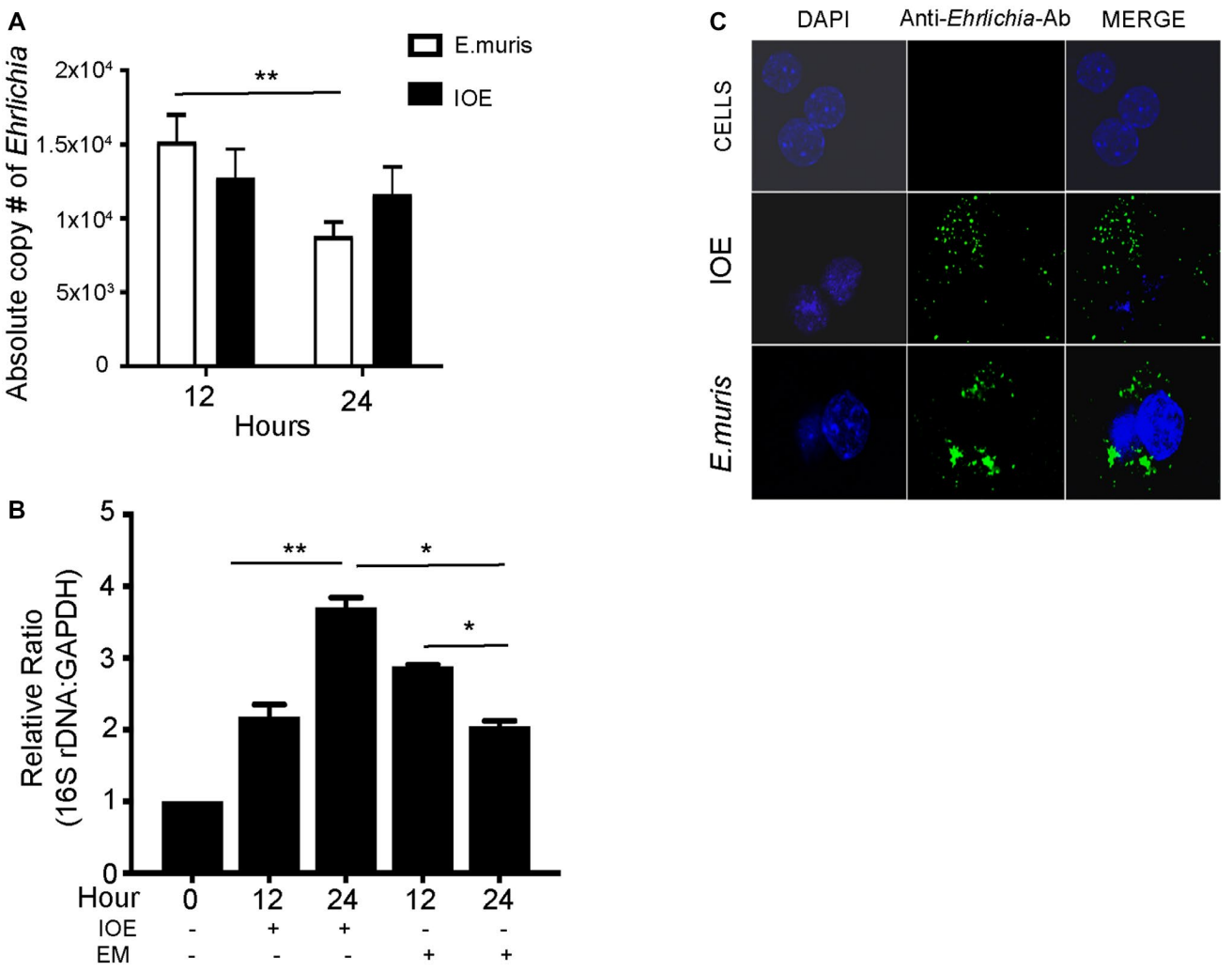

FIG. 1. *Ehrlichia* invade and replicate in HCs. (A) Absolute copy number of intracellular bacteria in murine HCs from WT mice infected with IOE and EM at 12 and 24 hours postinfection. (B) Relative expression of IOE and EM 16S rDNA, normalized to GAPDH, in order to detect viable bacteria in uninfected and infected WT HCs at 24 hours postinfection. (C) Immunofluorescence staining of primary HCs isolated from WT mice (WT-HCs) and infected *in vitro* with IOE or EM at an MOI of 5 and labeled with polyclonal anti-*Ehrlichia* antibodies. Scale bar 10 μm. Data are presented as mean ± SD (*$P < 0.05$, **$P < 0.01$) of mice/group and representative of three independent experiments. Abbreviation: Ab, antibody.

failure.[9] In contrast, infection with mildly virulent EM causes mild and self-limited disease with minimal hepatic pathology.[24] To determine how HCs contribute to the pathogenesis of *Ehrlichia*-induced liver damage, we first examined the HC response to IOE infection compared to EM infection. Primary HCs were isolated from naive WT mice and infected *in vitro* with IOE or EM at an MOI of 5. Analysis of total number of intracellular *Ehrlichia* by qPCR indicated that both IOE and EM enter and survive in HCs at 12 and 24 hours postinfection, although the number of EM but not IOE organisms significantly declined at 24 hours compared to 12 hours postinfection (Fig. 1A). Consistent with the qPCR of bacterial DNA, analysis of the number of live and replicating bacteria by 16S rDNA demonstrated a significantly higher number of replicating bacteria in IOE-infected HCs at 24 hours when compared to 12 hours ($P < 0.01$) while HCs were able to control the EM infection at 24 hours (Fig. 1B). The difference between the number of intracellular IOE and EM in HCs at 24 hours is less likely due to prolonged internalization of IOE

from the extracellular environment because we did not detect extracellular EM or IOE organisms in the HC culture supernatant at 12 and 24 hours after infection (data not shown). Immunofluorescence staining of cells with polyclonal cross-reactive anti-*Ehrilchia* antibodies demonstrated internalization of both EM and IOE organisms in HCs at 24 hours postinfection (Fig. 1C). These data suggest that IOE are able to evade host response and replicate within HCs compared to EM.

HCs ARE A CELLULAR SOURCE OF IFNβ AND CHEMOKINES DURING FATAL IOE INFECTION

Recent studies by us and other investigators have defined a central role for IFN-I in severe and fatal ehrlichiosis in mice infected with IOE.[14,19,25] To determine whether HCs contribute to IFNβ production and dysregulated production of cytokines and chemokines, we compared responses among uninfected, IOE-infected, and EM-infected HCs at 24 hours postinfection. Compared to uninfected and EM-infected HCs, we detected significant secretion of IFNβ by IOE-infected HCs at the protein level as measured by ELISA ($P < 0.001$)(Fig. 2A) and at the messenger RNA (mRNA) level as measured by qRT-PCR ($P < 0.001$ and <0.01, respectively) (Fig. 2B). mRNA quantification data indicated that infection of HCs with IOE significantly up-regulated IFNARs in HCs compared to uninfected and EM-infected HCs ($P < 0.05$) (Fig. 2C).

Based on these data and the findings that IFNAR signaling on nonhematopoietic cells plays a role in bacterial infection and the development of *Ehrlichia*-induced sepsis,[14,19,26,27] we hypothesized that binding of myeloid cell-derived IFN-I cytokines to IFNARs on HCs could mediate dysregulated inflammation and immunopathology. To test this hypothesis, HCs were infected with virulent IOE in the presence or absence of IFNβ and measured HC responses. IOE infection alone significantly increased expression of IFN regulatory factor 3 (IRF3) ($P < 0.05$) but not IRF7 (Fig. 2D,E) or IRF9 (data not shown). Exogenous IFNβ

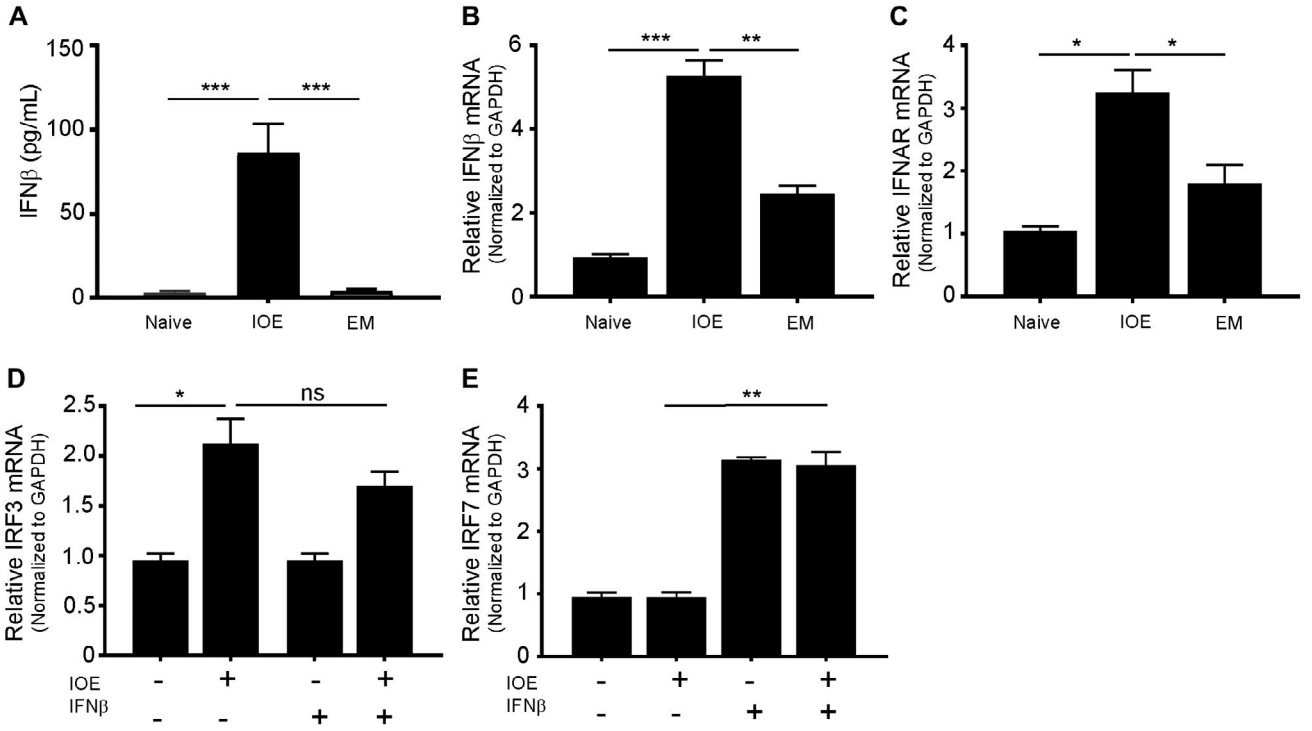

FIG. 2. IOE induces IFNβ and IFNAR in primary HCs. Uninfected or infected WT-HCs *in vitro* with IOE in the presence or absence of rIFNβ, and IFN-I responses at 24 hours postinfection. (A) Levels of secreted IFNβ measured by ELISA. (B,C) mRNA expression of IFNβ and IFNAR, respectively, measured by RT-qPCR. (D,E) Relative mRNA expression of IRF3 and IRF7, respectively, in IOE-infected WT-HCs following exogenous stimulation with rIFNβ. Data are representative of three independent experiments. All results presented as mean ± SD (*$P < 0.05$, **$P < 0.01$, ***$P < 0.001$). Abbreviation: ns, not significant.

stimulation did not increase IRF3 further compared to infection alone. On the other hand, rIFNβ stimulation of uninfected or IOE-infected HCs significantly triggered up-regulation of IRF7 ($P < 0.01$) compared to unstimulated controls (Fig. 2E), suggesting that IOE infection alone does not induce the expression of IRF7.

We next examined whether HCs contribute to excessive production of proinflammatory cytokines and chemokines, which is a major pathognomonic finding during fatal infection in mice and humans. Our data showed HCs infected with either IOE or EM did not produce significant levels of inflammatory cytokines tumor necrosis factor alpha, IL-12, IL-4, IL-5, IL-6, or IL-10 compared to uninfected HCs (data not shown). On the other hand, IOE-infected HCs produced significantly higher levels of granulocyte-macrophage colony-stimulating factor (GM-CSF; $P < 0.001$), macrophage inflammatory protein 1 alpha (MIP1α; $P < 0.01$), IFNγ-induced protein 10/chemokine (C-X-C motif) ligand 10 (CXCL10), monokine induced by gamma (MIG)/CXCL9, keratinocyte-derived chemokine (KC)/CXCL1, regulated upon activation, normal T-cell expressed, and secreted (RANTES)/chemokine (C-C motif) ligand 5 (CCL5) ($P < 0.001$), vascular endothelial growth factor ($P < 0.05$), and monocyte chemoattractant protein 1 (MCP1)/CCL2 compared to uninfected and EM-infected HCs (Fig 3A-H). Notably, rIFNβ stimulation of IOE-infected HCs resulted in a significant increase in the production of GM-CSF (neutrophil chemoattractant and growth factor) and MIP1α (macrophage chemoattractant) ($P < 0.0001$ and $P < 0.001$, respectively) when compared to unstimulated infected HCs (Fig. 4A,B). We did not observe a significant increase in the secretion of other chemokines by IOE-infected HCs following IFNβ stimulation (Fig. 4C-E). Taken together, these data suggest that HCs are a major source of several chemokines associated with fatal infection.

IFN-I SIGNALING INDUCES ACTIVATION OF CANONICAL AND NONCANONICAL INFLAMMASOME PATHWAYS IN IOE-INFECTED HCs

We next examined whether IOE infection triggers inflammasome activation in HCs and if this response was regulated by IFNAR signaling and measured markers of canonical and noncanonical inflammasome pathways. IOE infection significantly enhanced mRNA expression of caspase-1, IL-1β, and caspase-11 in HCs compared to uninfected cells (Fig. 5A-C). Additional rIFNβ stimulation of HCs significantly up-regulated mRNA expression of caspase-1 ($P < 0.01$), IL-1β ($P < 0.01$), and caspase-11 ($P < 0.00.1$) in both uninfected and IOE-infected HCs compared to unstimulated control cells with or without infection (Fig. 5A-C). To validate mRNA data at the protein level, we measured expression of active caspase-1 and caspase-11 by immunoblot. Infection of HCs induced activation of active caspase-1 and caspase-11 when compared to uninfected cells. Although stimulation of uninfected HCs with rIFNβ was higher than unstimulated and uninfected controls, IOE infection of IFNβ-stimulated cells further increased expression of active caspase-1 and caspase-11 rIFNβ (Fig. 5D,E). This synergistic effect of infection and paracrine IFNAR signaling also resulted in significant secretion of IL-1β (Fig. 5F) as well as pyroptotic cell death marked by significant increase in lactate dehydrogenase (LDH) release when compared to IOE infection alone, rIFNβ alone, or uninfected/unstimulated cells (Fig. 5G). Together, these data suggest that IOE infection triggers significant canonical and noncanonical inflammasome activation marked by cleavage of caspase-1, caspase-11, IL-1β secretion, and pyroptosis following paracrine IFNAR signaling.

EHRLICHIA INFECTION INDUCED HMGB1 RELEASE IS MEDIATED BY IFNAR SIGNALING

Activation of caspase-11 during gram-negative bacterial infection induces secretion of HMGB1.[28] HMGB1 is a nuclear protein that acts as a DAMP when translocated to the cytosol and is secreted actively or passively following necrotic cell death during many inflammatory diseases. To determine the contribution of HMGB1 to *Ehrlichia*-induced sepsis, we first measured the serum levels of HMGB1 in IOE and EM-infected WT mice on day 7 post-infection. Compared to uninfected and EM-infected mice (mild disease), IOE-infected mice (fatal disease) had significantly higher serum levels of HMGB1 ($P < 0.01$) (Fig. 6A), suggesting that systemic

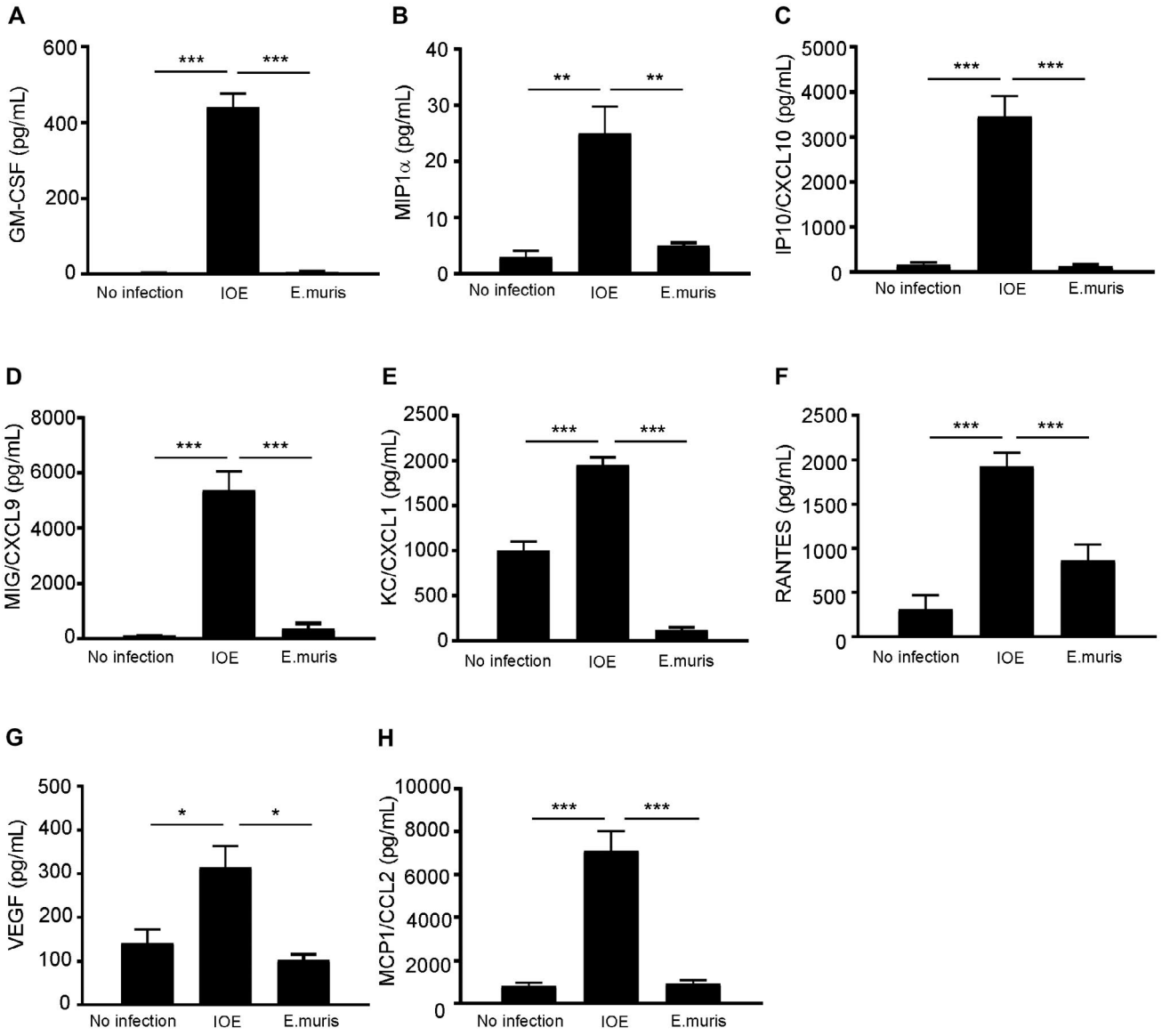

FIG. 3. Chemokine production by HCs following IOE and EM infection. WT HCs were infected with IOE and EM at an MOI of 5, and HC responses were analyzed at 24 hours postinfection. Significant secretion of cytokines, presented in pg/mL, were quantified by ELISA, including (A) GM-CSF, (B) MIP1α, (C) IP10/CXCL10, (D) MIG/CXCL9, (E) KC/CXCL1, (F) RANTES, (G) VEGF, and (H) MCP1/CCL2, in HC culture supernatant infected with IOE compared to uninfected and untreated controls. Data are representative of three independent experiments. All results presented as mean ± SD (*$P < 0.05$, **$P < 0.01$, ***$P < 0.001$). Abbreviations: IP10, interferon-gamma-induced protein 10; VEGF, vascular endothelial growth factor.

HMGB1 production is associated with a fatal ehrlichiosis. Next, we examined the contribution of hepatic IFNAR signaling to HMGB1 production by analyzing HMGB1 cytosolic translocation and secretion in HCs following *in vitro* infection with IOE in the presence or absence of rIFNβ. We detected significant cytosolic translocation of HMGB1 in IOE-infected HCs following stimulation with IFNβ compared to IOE alone or uninfected cells ($P < 0.01$) (Fig. 6B). Quantitative analysis of nuclear HMGB1 by confocal microscopy demonstrated a significantly higher level of HMGB1 in the nucleus of IOE-infected cells and uninfected cells stimulated with IFNβ compared to the level of nuclear HMGB1 in uninfected HCs or infected cells stimulated with IFNβ (Fig. 6C). This result further confirmed cytosolic translocation in

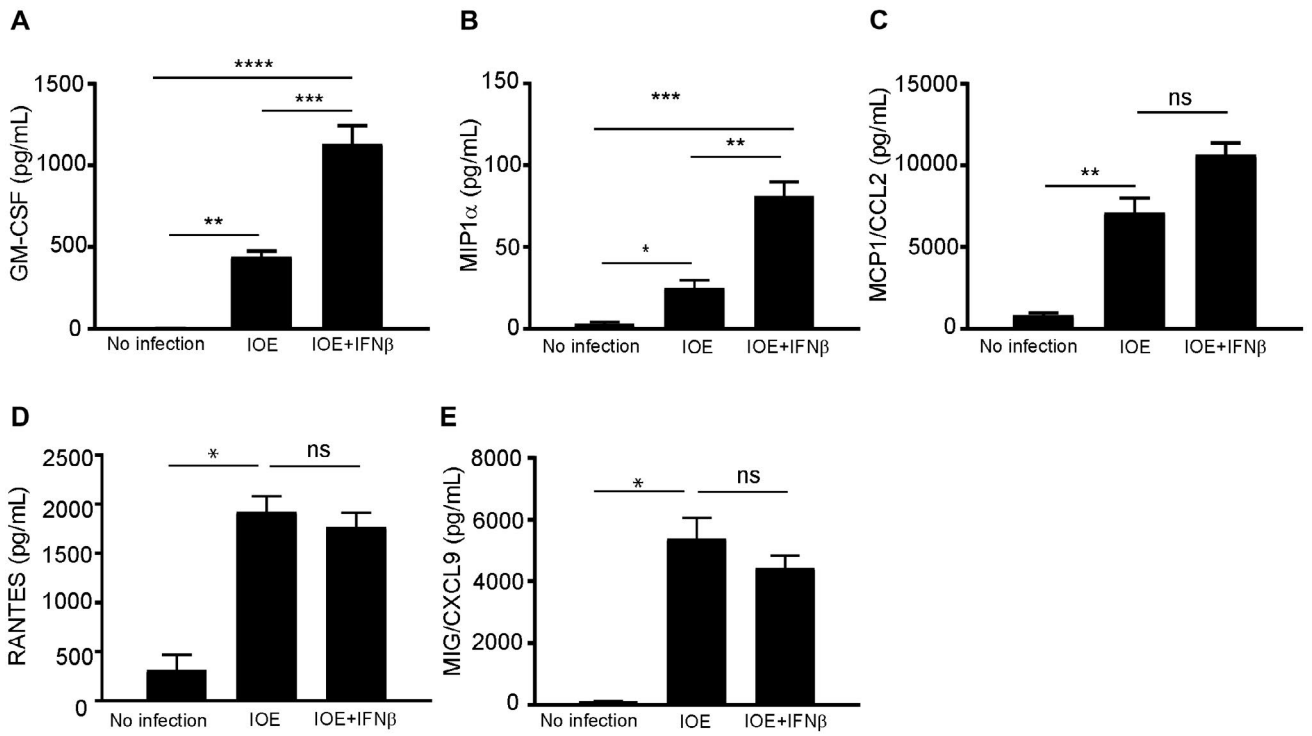

FIG. 4. Chemokine production by HCs following IOE infection and IFNβ stimulation. WT-HCs were infected with IOE at an MOI of 5 with and without IFNβ, and HC responses were analyzed at 24 hours postinfection. Significant secretion of cytokines quantified by ELISA and presented in pg/mL, including: (A) GM-CSF, (B) MIP1α following IOE infection and IFNβ stimulation. No significant difference was observed for (C) MCP1/CCL2, (D) RANTES, and (E) MIG/CXCL9, between IOE-infected and IOE-infected-IFNβ stimulated HCs. All results presented as mean ± SD (*$P < 0.05$,**$P < 0.01$, ***$P < 0.001$, ****$P < 0.0001$). Abbreviation: ns, not significant.

the former conditions. Increased cytosolic translocation of HMGB1 in infected cells following paracrine IFNAR signaling was consistent with higher mRNA expression of HMGB1 compared to controls (Fig. 6D).

We next examined whether paracrine IFNARs promote HMGB1 secretion and whether IFNAR-mediated HMGB1 secretion is dependent on caspase-11. To this end, we measured HMGB1 secretion from IOE-infected WT and caspase-11-deficient (caspase-$11^{-/-}$) primary HCs cultured with or without exogenous IFNβ. We found that IFNβ stimulation of IOE-infected WT HCs induced significantly higher secretion of HMGB1 and IL-1α compared to unstimulated but infected cells (Fig. 6E,F). Notably, caspase-11 deficiency significantly decreased HMGB1 and IL-1α secretion from infected HCs stimulated with IFNβ compared to WT controls (Fig. 6E,F). Inhibition of caspase-1 activation in WT HCs also resulted in an attenuated extracellular level of HMGB1 and IL-1α, although the effect was less remarkable compared to the impact of caspase-11 deficiency. Combined inhibition of caspase-11 and caspase-1 pathways in IOE-infected HCs stimulated with IFNβ resulted in complete abrogation of HMGB1 secretion (Fig. 6E,F). Together, these data suggest that IFNAR-mediated HMGB1 secretion is mainly dependent on caspase-11.

IFNβ SIGNALING PROMOTES BACTERIAL REPLICATION IN HCs DURING *EHRLICHIA* INFECTION

We have previously shown that the increased resistance of IFNAR-deficient mice is associated with decreased bacterial burden in the liver.[19] Thus, we hypothesized that IFNAR signaling could promote bacterial replication in HCs. To test this hypothesis, we measured the total number of live intracellular IOE in primary HCs by qPCR. *In vitro* stimulation

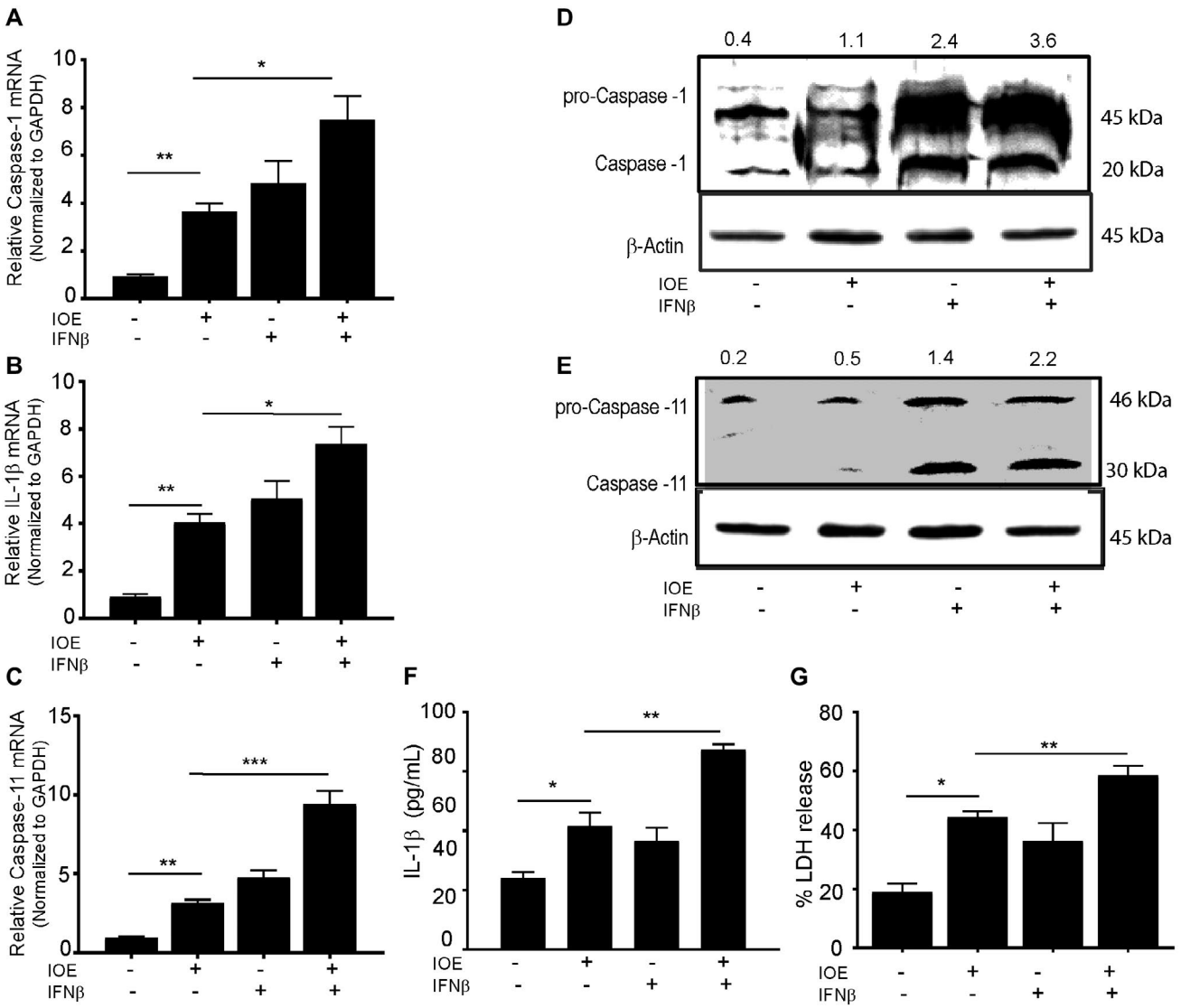

FIG. 5. Paracrine IFNAR signaling promotes caspase-11 activation in infected HCs. WT-HCs uninfected or infected with IOE *in vitro* in the presence or absence of IFNβ. (A-C) Inflammasome activation was assessed at 24 hours postinfection based on mRNA expression of caspase-1, IL-1β, and caspase-11 and quantified by RT qPCR. (D,E) Representative immunoblot analysis of caspase-1 and caspase-11 proteins; β-actin was used as the loading control. (F) Level of IL-1β in culture supernatant measured by ELISA and presented in pg/mL. (G) LDH release as marker of pyroptosis was measured in uninfected and infected HCs with and without IFNβ (500 IU/mL) and presented as a percentage. Data from *in vitro* experiments are representative of three independent experiments. All results presented as mean ± SD (*$P < 0.05$, **$P < 0.01$, ***$P < 0.001$).

of IOE-infected HCs with rIFNβ significantly enhanced bacterial survival and replication as measured by qPCR of the 16S rDNA at 24 hours postinfection compared to unstimulated uninfected HCs ($P < 0.01$). This effect was abrogated when infected and stimulated cells were treated with anti-IFNAR blocking antibodies (Fig. 7A) ($P < 0.05$), confirming that indeed IFNAR signaling is responsible for the increased number of intracellular *Ehrlichia*.

IFNβ SIGNALING INCREASES AUTOPHAGY INDUCTION AND AUTOPHAGIC FLUX IN HCs DURING *EHRLICHIA* INFECTION

Because *Ehrlichia* uses autophagy proteins for their own survival and replication, we hypothesized that IFNAR may enhance bacterial replication in IOE-infected HCs by inducing autophagy. To test this

hypothesis, we measured the number of LC3 puncta (as a marker of autophagosome formation) by confocal microscopy as well as conversion of LC3I to LC3II by immunoblot. Confocal microscopy analysis showed that IOE infection of HCs significantly increased the number of LC3 puncta/cells when compared to

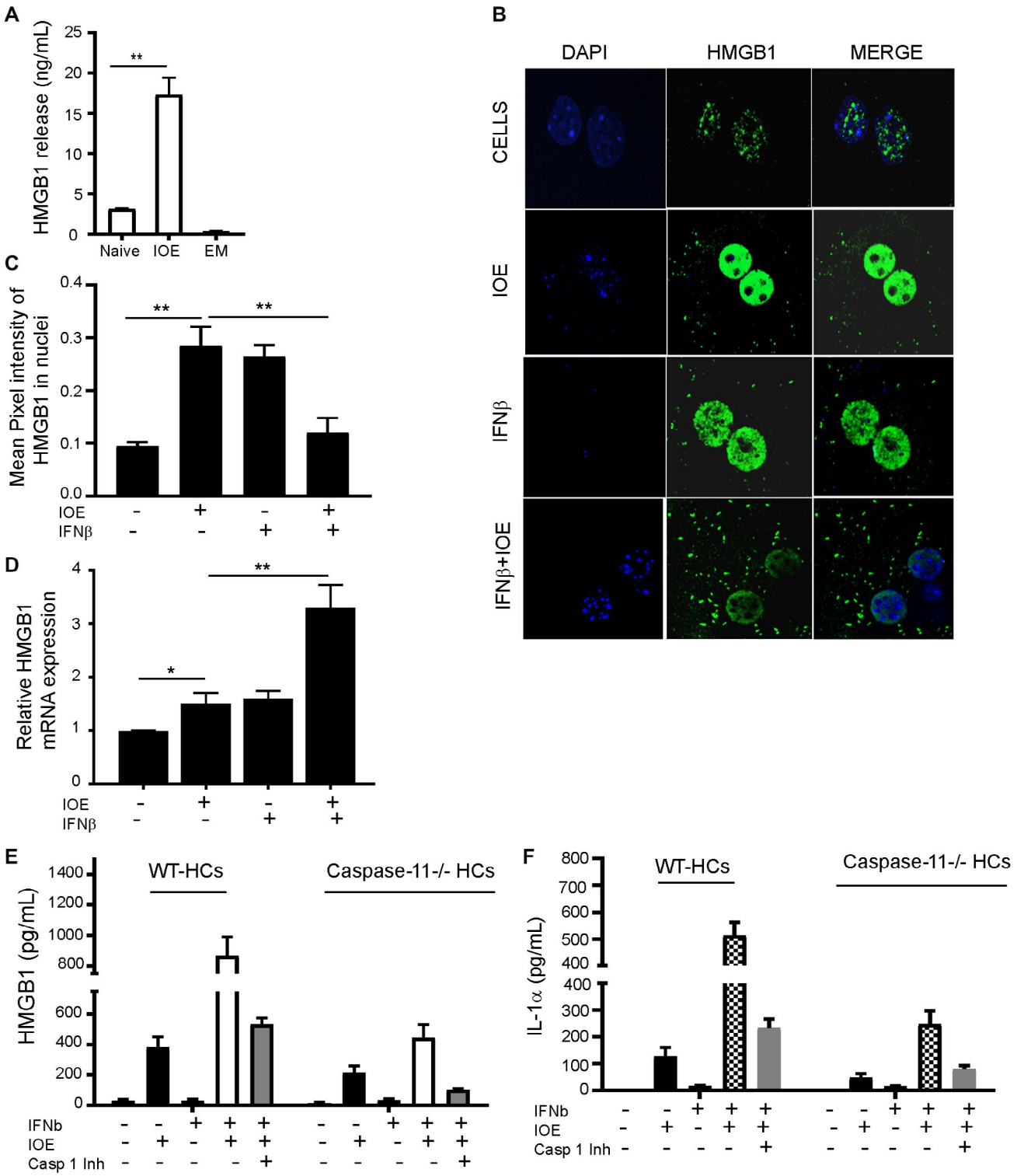

FIG. 6. HMGB1 release during fatal *Ehrlichia* infection is mediated by IFNAR signaling. (A) Serum HMGB1 levels for infected or uninfected mice with no treatment. (B) Immunofluorescence staining of cells at 24 hours postinfection using anti-HMGB1 antibodies showing translocation of HMGB1 in IOE-infected HCs following paracrine IFNβ stimulation. Scale bar 10 μm. (C) Quantitation of mean pixel intensity of HMGB1 in nuclei of uninfected and IOE-infected cells in the presence or absence of IFNβ. (D) Relative expression of HMGB1 mRNA in cell lysates from the indicated culture conditions. WT HCs and caspase-11$^{-/-}$-deficient HCs were infected with IOE in the presence and absence of IFNβ (500 IU/mL) and caspase-1 inhibitor (10 μm/mL), individually or together. The culture supernatant of HCs was used to determine by ELISA the level (pg/mL) of (E) HMGB1 and (F) IL-1α. Data from *in vitro* experiments are representative of three independent experiments. All results presented as mean ± SD (*$P < 0.05$, **$P < 0.01$). Abbreviations: Casp, caspase; Inh, inhibitor.

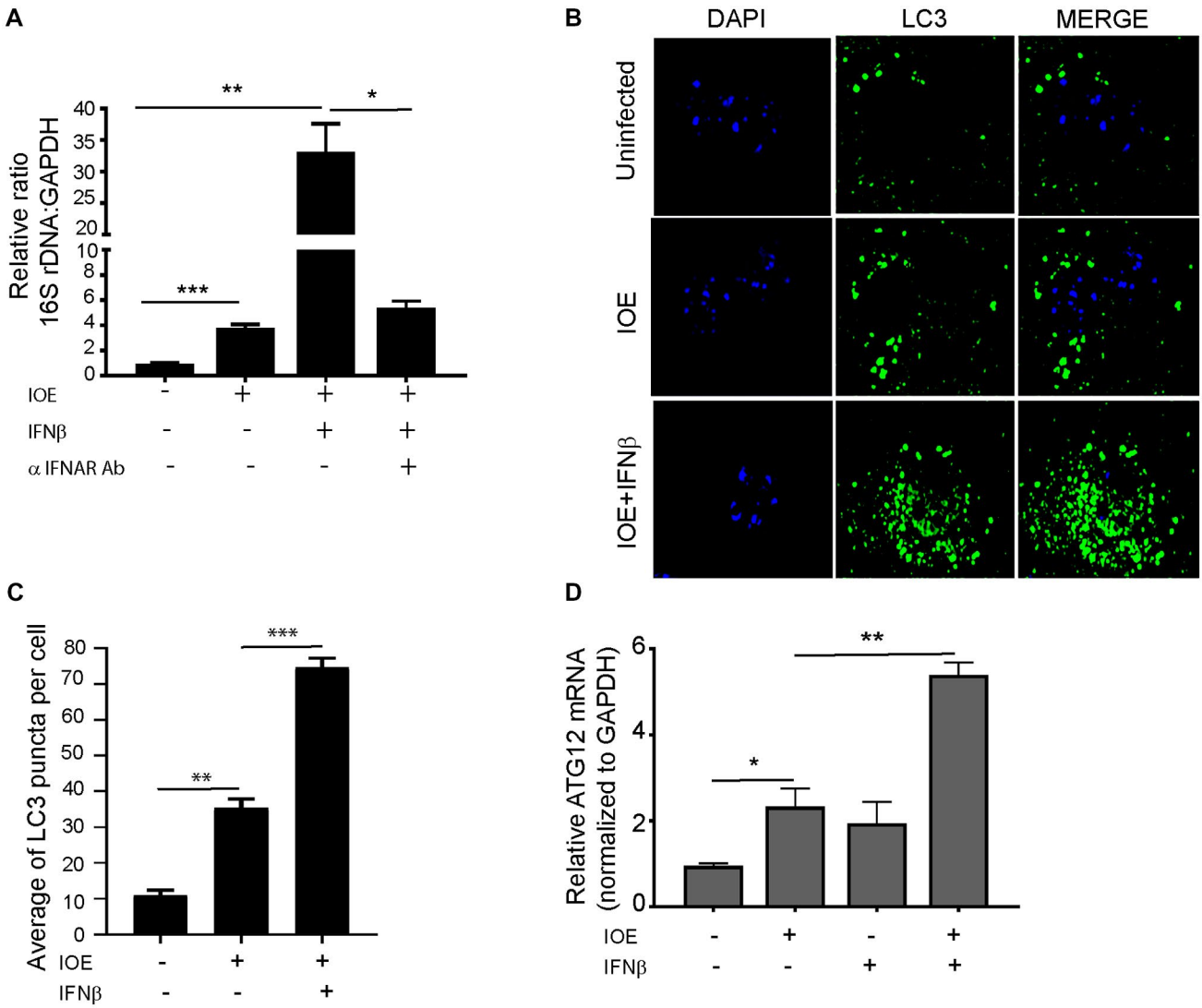

FIG. 7. Paracrine IFNAR signaling enhances autophagy and bacterial replication. (A) Relative expression of IOE 16S rDNA for detecting viable bacteria, normalized to GAPDH, in uninfected and infected WT HCs with and without IFNβ (500 IU/mL) and in the presence or absence of anti-IFNAR monoclonal antibody. (B) Immunofluorescence staining showing higher LC3B puncta in infected HCs stimulated with IFNβ (500 IU/mL); cells stained with anti-LC3 antibodies and DAPI for nuclear localization. Scale bar 10 μm. (C) Average of LC3 puncta per HCs with IOE and stimulated with IFNβ (500 IU/mL) compared to the corresponding controls. (D) Relative quantification of ATG12 by RT-qPCR and normalized to GAPDH. All results are presented as mean ± SD (*$P < 0.05$, **$P < 0.01$, ***$P < 0.001$) from three independent *in vitro* experiments. Abbreviation: Ab, antibody.

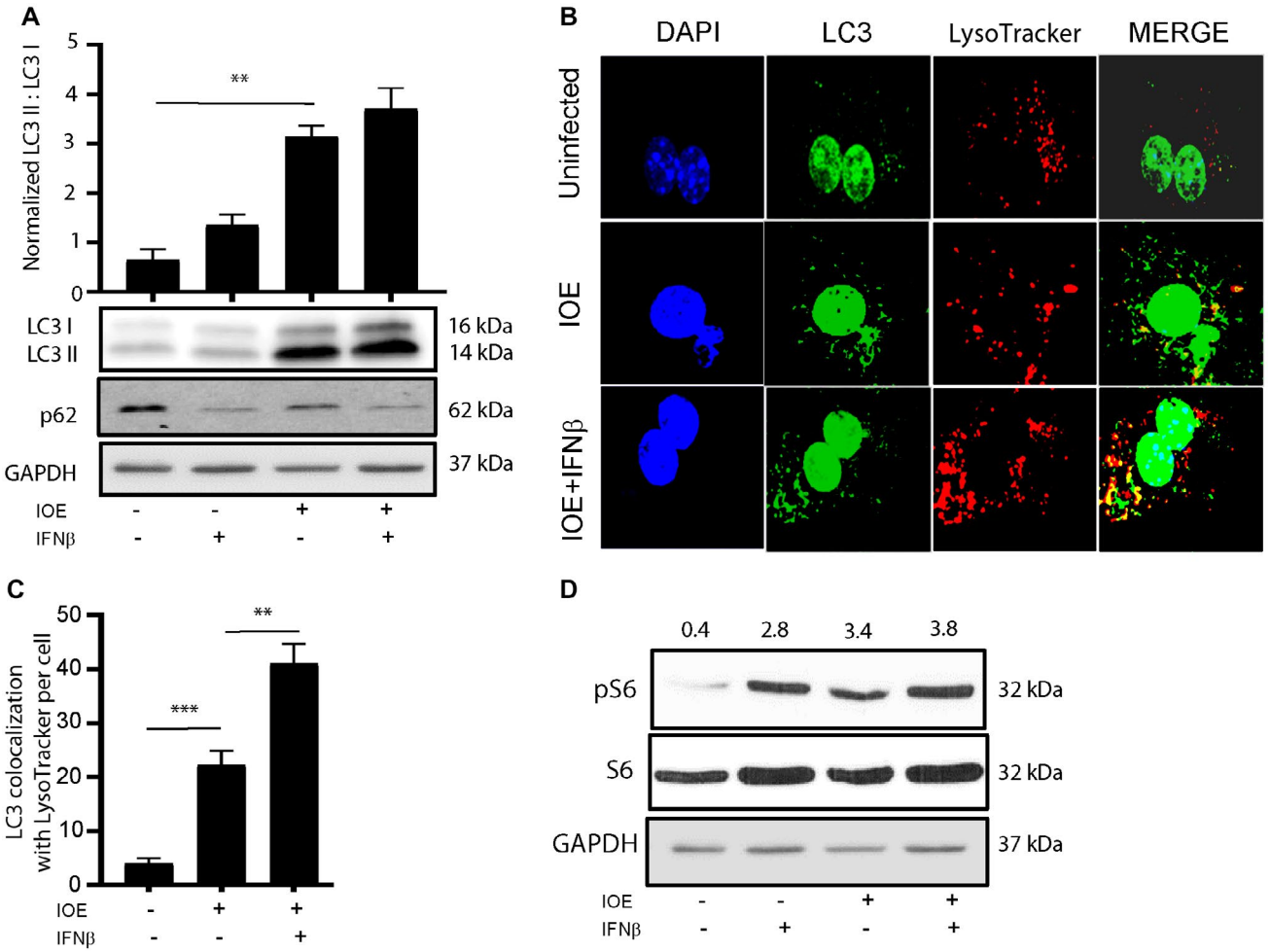

FIG. 8. IOE infection induces mTORC1-independent autophagy in HCs following exogenous IFNβ stimulation. (A) Representative immunoblot analysis of LC3I/II and p62/SQSTM1 in uninfected and IOE-infected WT HCs cultured with or without IFNβ at 24 hours postinfection; GAPDH used as loading control. Density of bands is quantified and normalized to GAPDH expression. (B) Immunofluorescence staining with LC3 (green) and LysoTracker (red) showing higher colocalization of LC3 and LysoTracker (yellow) puncta in IOE-infected HCs stimulated with IFNβ (500 IU/mL). Cells stained with DAPI (blue) for nuclear localization. Scale bar 10 μm. (C) Quantification of LC3 with LysoTracker per cell. (D) Immunoblot showing expression of pS6 and total S6, a downstream target of mTORC1 activation; GAPDH used as loading control. Data in (A,C) are presented as mean ± SEM from three different experiments (**$P < 0.01$, ***$P < 0.001$).

uninfected cells, with a further increase in the number of LC3 puncta/cells following exogenous stimulation with rIFNβ (Fig. 7B,C). Furthermore, mRNA expression of autophagy-related 12 (ATG12), a major autophagy protein that initiates autophagosome formation, was significantly higher in IOE-infected WT HCs following rIFNβ stimulation compared to unstimulated uninfected controls at 24 hours postinfection (Fig. 7D) ($P < 0.05$). Consistent with the immunofluorescence data, we detected a significant increase in LC3II expression and higher LC3II/I ratio by immunoblot in IOE-infected HCs following IFNβ stimulation when compared to uninfected or infected HCs cultured without rIFNβ (Fig. 8A). The accumulation of LC3II in IOE-infected and IFNβ stimulated HCs could be due to enhanced autophagosome formation/induction or a reduced degradation of autophagic cargo. To distinguish between these events, we analyzed autophagic flux by measuring the level of p62/SQSTM1, a selective autophagy adaptor/receptor that binds to ubiquitinylated proteins and damaged organelles to target them to autophagosome-lysosomal

compartments for degradation. The total cellular p62/SQSTM1 expression levels inversely correlated with autophagic flux and activity. Compared to uninfected HCs, there was slightly less accumulation of p62 in IOE-infected HCs cultured with or without IFNβ, although less accumulation was detected in infected cells following IFNβ stimulation (Fig. 8A). These data suggest that autophagy flux is enhanced in both conditions. Similarly, immunofluorescence staining of LC3B showed that IOE-infected HCs had increased LC3B colocalization with lysosomes (stained by LysoTracker Red) following IFNβ stimulation when compared to uninfected and unstimulated IOE-infected HCs (Fig. 8B,C). These data further confirm that increased LC3II in infected HCs following paracrine IFNAR signaling is due to enhanced autophagy induction but not to blocked flux.

Recently, we demonstrated that induction of autophagy in macrophages is negatively regulated by mTORC1 following infection with IOE.[10] To examine if similar regulation occurs in HCs, we measured mTORC1 activation by immunoblotting. We found that IOE infection induced mTORC1 activation following stimulation with rIFNβ, as marked by pS6, when compared to the uninfected unstimulated cells (Fig. 8D). Together, these results suggest that autophagy regulation in HCs infected with virulent *Ehrlichia* is mTORC1 independent.

HEPATOCYTE-SPECIFIC CASPASE-11 AND CASPASE-1 ACTIVATION *IN VIVO* CORRELATE WITH FATAL OUTCOME

We and others have demonstrated substantial IFNβ production in the liver and spleen of IOE-infected mice that correlates with liver injury, multiorgan failure, sepsis, and death on days 8-10 postinfection.[19,20] In contrast, mild and self-limited disease in EM-infected mice correlate with lack of IFN-I response. To validate our *in vitro* data, we isolated primary HCs from the livers of IOE- and EM-infected mice on day 7 postinfection. Our immunoblot data showed that primary HCs from IOE-infected mice exhibit activation of mTORC1, as marked by expression of pS6, as well as cleavage/activation of caspase-11 and caspase-1 compared to HCs from uninfected and EM-infected mice (Fig. 9A-C). Together, these data indicate that hepatic IFNAR signaling mediates caspase-1/caspase-11 activation, which in turn causes release of HMGB1 and inflammatory cell death, which cause liver injury and sepsis following lethal infection.

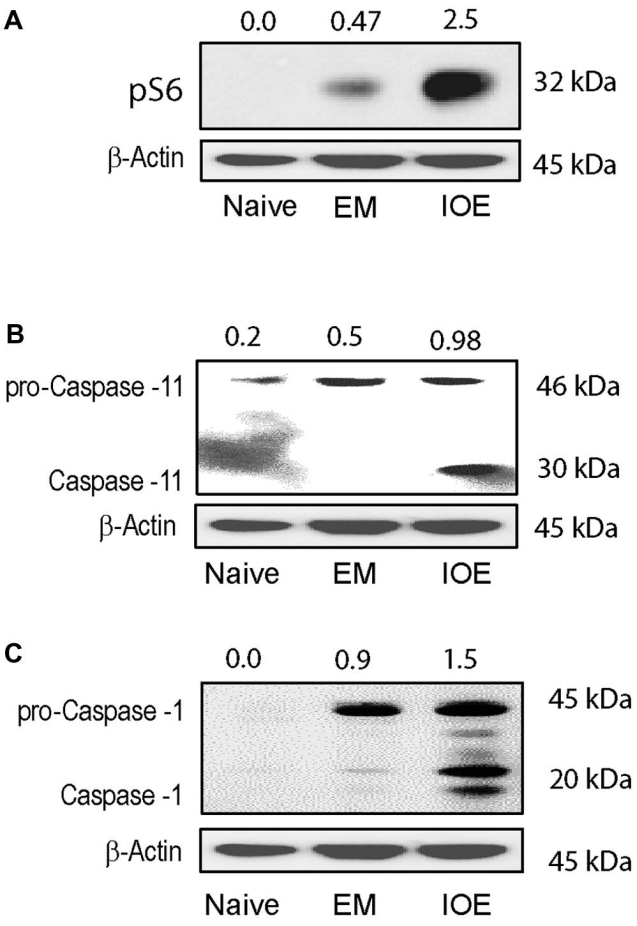

FIG. 9. *In vivo* validation of IFNAR and paracrine IFNβ roles in the pathogenesis of *Ehrlichia*-induced liver injury. *In vivo* western blot analysis of proteins extracted from primary HCs isolated from IOE- and EM-infected C57BL/6 mice and naive control. (A-C) Representative immunoblot analysis of pS6, caspase-11, and caspase-1 proteins; β-actin used as loading control.

Discussion

The liver is a major site of pathology and infection in patients with *Ehrlichia*-induced sepsis.[14] The mechanism by which *Ehrlichia* infection induces liver injury remains unclear. Using two *Ehrlichia* species that cause mild/self-limited disease or fatal ehlichiosis in mice and humans, we uncovered in this study an important role for HCs and in particular hepatic

IFN-I signaling in mediating *Ehrlichia*-induced liver injury. Several laboratories including our own have shown that IFNAR signaling plays a pathogenic role in the pathogenesis of fatal ehrlichiosis by promoting inflammasome activation and liver injury.[10,19,20] The expression of IFNAR in nonhematopoietic cells is a key player in bacterial replication and fatal ehrlichiosis where IFNβ production is mainly mediated by plasmacytoid dendritic cells and monocytes.[20] To mimic the *in vivo* cross-talk between myeloid cells and HCs during fatal *Ehrlichia* infection, we examined the HC response to IOE infection following exogenous/paracrine stimulation with IFNβ. Here, we show that paracrine IFNAR signaling on HCs mediates *Ehrlichia*-induced sepsis by mechanisms involving activation of a noncanonical inflammasome pathway mediated by caspase-11, resulting in cytosolic translocation of HMGB1 and active secretion from HCs.

Our data suggest that the noncanonical caspase-11-mediated inflammasome pathway is the key mechanism that accounts for dysregulated inflammasome activation following IFNAR signaling and subsequent liver damage. This conclusion is further supported by our previous study showing that lack of caspase-11 in IFNAR$^{-/-}$ mice was linked to minimal liver pathology and heightened resistance to fatal ehrlichiosis while lack of caspase-1 in caspase-1 knockout mice did not alter susceptibility to fatal disease compared to IOE-infected WT mice.[19] The lack of caspase-11 in IOE-infected IFNAR$^{-/-}$ mice resulted in decreased serum level of IL-1β mice, suggesting that caspase-11 promotes activation of caspase-1-dependent IL-1β production. In this study, we examined whether the IFNAR–caspase-11 axis is upstream of HMGB1 and IL-1α. Our data demonstrate a reduced secretion of HMGB1 and IL-1α in IOE-infected caspase-11-deficient HCs compared to infected WT cells or IOE-infected HCs treated with caspase-1 inhibitor. Deletion of caspase-11 along with inhibition of caspase-1 significantly suppressed the secretion of both HMGB1 and IL-1α. We also found that infected HCs undergo pyroptosis (caspase-11-dependent cell death) following exogenous IFNβ stimulation, as indicated by LDH release (Fig. 5). We further validated these *in vitro* data by examining activation of caspase-11 and caspase-1 in *in vivo*-infected HCs harvested from IOE (a fatal model with heightened IFN-I response) and EM-infected mice (a model that lacks IFN-I response). Our data show a strong correlation between IFNAR signaling, inflammation, caspase-1–HMGB1 axis, and fatal *Ehrlichia*-induced liver injury and sepsis. Together, our study suggests that IFNAR induces caspase-11 activation during a fatal infection, which in turn mediates caspase-1 activation and subsequent IL-1β production as well as caspase-11/1-dependent HMGB1 secretion and pyroptotic cell death.

How HMGB1 contributes to *Ehrlichia*-induced liver injury and sepsis remains elusive. However, we argue that HMGB1 contributes to both immune-mediated liver damage as well as defective immunity and enhanced bacterial survival and replication. In support of HMGB1-mediated liver damage, our data (Fig. 6A) demonstrate that development of liver injury and fatal sepsis in IOE-infected mice is associated with high serum levels of HMGB1. On the other hand, lack of liver damage and development of mild diseases in EM-infected mice correlate with undetectable HMGB1 in circulation (Fig. 6A). Extracellular hepatic HMGB1 could also bind to the receptor for advanced glycation end products (RAGE) on uninfected cells (macrophages or HCs), which then triggers caspase-1 activation and pyroptosis as suggested by other studies.[29-31] Our data are consistent with other studies showing that genetic deletion of *Hmgb1* or inhibition with HMGB1-neutralizing antibodies protects mice from lethal endotoxemia and sepsis.[30,31] Notably, our data show that cytosolic translocation of HMGB1 correlates with autophagy induction. We and others have shown that *Ehrlichia* exploit the autophagy process to obtain nutrients for their own survival and replication.[10,32,33] How intracellular HMGB1 induces autophagy in our model is unknown. However, as suggested by others, translocation of HMGB1 to the cytosol following stressful stimuli may promote autophagy by direct interaction with beclin-1 (a key protein that initiates autophagosome formation), which results in separation of beclin-1 from Bcl2 apoptosis regulator (Bcl2).[29,30] This HMGB1–beclin1 complex is controlled at the transcriptional, posttranscriptional, and posttranslational level and is positively regulated by unc-51-like autophagy activating kinase 1 (Ulk1) and mitogen-activated protein kinase (MAPK).[29-32] Our unpublished data suggest that MAPK plays a role in the induction of autophagy in HCs following IOE infection, as evidenced by phosphorylation and activation of the p38 MAPKs (data not shown). The findings that IOE infection induces autophagy

following exogenous IFNβ stimulation despite activation of negative regulator mTORC1 (Fig. 7) suggests that induction of autophagy under these conditions is mTORC1 independent and may occur by a noncanonical pathway mediated by MAPK. On the other hand, extracellular/reduced HMGB1 may induce autophagy through interaction with RAGE.[29,30] Together, our data suggest that IFNAR signaling in HCs enhances autophagy by HMGB1. These data explain our previous *in vivo* studies[19] showing a protective immunity and decreased bacterial burden in IOE-infected *Ifnar*$^{-/-}$ mice compared to IOE-infected WT mice.

Our data indicate that IOE induced IFNβ secretion from HCs and involved IRF3 signaling (Fig. 2). However, the exact upstream receptor of IRF3 remains elusive. We speculate that this IFN-I production may be mediated by cytosolic receptors, such as stimulator of interferon genes (STING) and retinoic acid-inducible gene-I (RIG-1), that are involved in the IFN-I response.[34] These receptors could be triggered by *Ehrlichia* tandem repeat proteins (TRPs), such as TRP75 and TRP120, that are secreted into cytosol and are known to interact with a diverse group of human proteins associated with innate responses, multiple metabolic processes, and signal transduction.[14,35,36] Alternatively, bacterial or mitochondrial DNA can bind to toll-like receptor 9 (TLR9), another upstream receptor that is involved in production of IFN-I cytokines. This possibility is based on our study showing that the TLR9–MYD88 pathway plays a role in inflammasome activation in macrophages and IOE-induced liver injury.[10]

Our study also showed that infection of HCs with virulent IOE induced significantly increased levels of several chemokines known to promote infiltration of immune cells in the liver, including T cells, natural killer (NK)T cells, and neutrophils.[34] We have previously demonstrated that neutrophils play a pathogenic role in the host response to *Ehrlichia* as they promote excessive inflammation and induction of pathogenic cluster of differentiation (CD)8+ T cells.[11,37,38] We have also shown that secretion of inflammasome-dependent cytokine IL-18 and IL-18 signaling promote neutrophil expansion and migration to sites of infection.[15] These data suggest that chemokine production by HCs following IOE infection promotes migration and expansion of neutrophils, NKT cells, and CD8+ T cells in the liver following IFNβ/IFNAR signaling, causing sepsis and multiorgan failure.

Although our data are also consistent with a recent study by Deng et al,[39] demonstrating a role of HMGB1 in caspase-11-mediated injury, there are several differences between the two studies. First, the study by Deng et al. examined the role of the caspase-11–HMGB1 axis in liver injury caused by LPS of gram-negative bacteria. The data from their LPS model, although intriguing, cannot be generalized to hepatic infections caused by other gram-negative bacterial pathogens that harbor a plethora of other virulence factors known to activate multiple innate and adaptive immune signaling pathways. Our model system employs *Ehrlichia*, gram-negative bacteria that lack LPS yet trigger the deleterious caspase-11–HMGB1 axis and liver injury. The exact microbial ligand that triggers caspase-11 activation in our model remains elusive. However, *Ehrlichia* TRPs that are secreted by the type I secretion system[14,35,36] or *Ehrlichia* translocated factor-2 (Etf-2) that is secreted by the type IV secretion system into cytosol[40] are likely ligands or PAMPs that trigger inflammasome activation.[41,42] Additionally, our data suggest that DAMPs, such as mitochondrial (mt) DAMPs, are potential ligands that mediate canonical and noncanonical inflammasome activation.[41,42] Similar to our previous study examining macrophage response to IOE infection,[10] our unpublished preliminary data suggest that IOE induces metabolic reprogramming, oxidative stress, and mitochondrial dysfunction in HCs, which are associated with intracellular accumulation of mtDAMPs (e.g., reactive oxygen species, mtDNA, and cardiolipin) known to trigger inflammasome activation.[28,40-42] Such mitochondrial dysfunction is possibly induced further due to blocked mitophagy, as suggested by our recent study in macrophages.[10] Second, while Deng et al[39] suggest that HMGB1 directly interacts with LPS to mediate caspase-11-dependent pyroptosis in lethal sepsis, we demonstrate, for the first time, that the deleterious role of HMGB1 is induced only following IFN-I signaling by mechanisms described above and shown in Fig. 10. Finally, our data suggest cell-specific inflammasome activation during virulent IOE infection. In macrophages, IOE causes inhibition of autophagy by mTORC1 activation, which in turn causes inflammasome activation.[5] In contrast, IOE induces autophagy in HCs by mTORC1-independent pathways and is further enhanced by paracrine IFNAR signaling. The role of mTORC1

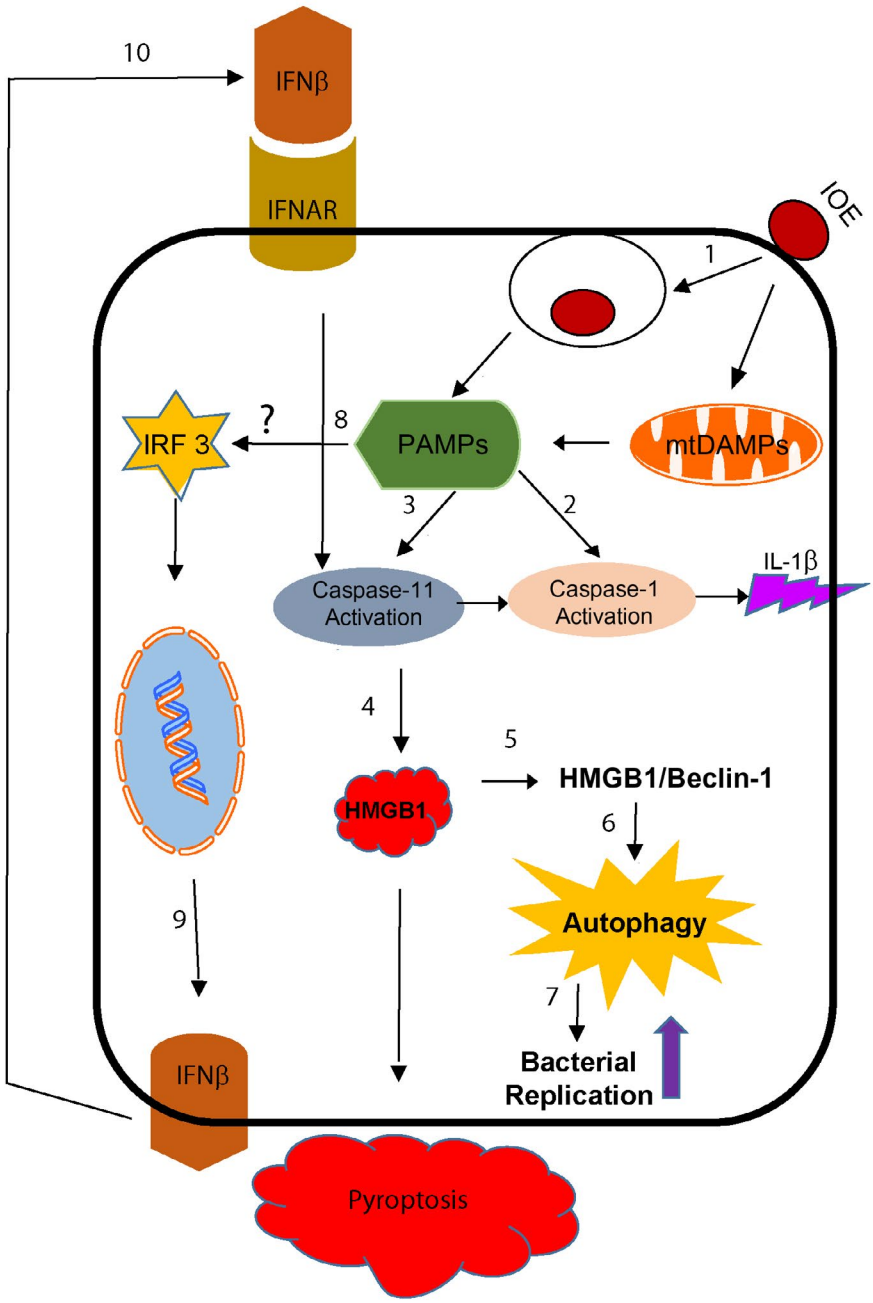

FIG. 10. Schematic model of IFNAR and paracrine IFNβ roles in the pathogenesis of *Ehrlichia*-induced liver injury. (1) IOE entry in HCs release cytosolic PAMPs and DAMPs (after induction of mitochondrial damage), which provide the first signal for activation of the (2) canonical (caspase-1-dependent) and (3) noncanonical (caspase-11-dependent) inflammasome pathways. (4) IFNAR signaling up-regulates expression of nuclear HMGB1 and its translocation to the cytosol through a common step with the noncanonical pathway of capsase-11. HMGB1 can then induce apoptosis or pyroptosis of adjacent cells. (5) Cytosolic HMGB1 also binds to beclin-1, which in turn (6) induces autophagosome formation and induction of autophagy. (7) As *Ehrlichia* hijack autophagy proteins for their survival, the formation of autophagosome enhances intracellular bacterial survival and replication. (8) A second signal for significant activation of caspase-11 and secretion of proinflammatory cytokines, including (9) IFNβ by activation of nuclear factor kappa B (not shown) is through (10) the binding of IFNβ to IFNAR, which can be considered a positive feedback loop in this model. Furthermore, caspase-11 activation is expected to promote further activation of caspase-1 and consequently the cleavage and secretion of mature IL-1β.

activation in the pathogenesis of ehrlichiosis is not yet understood. mTORC1 activation in HCs may enable obligate intracellular *Ehrlichia* to survive and replicate and induce inflammatory responses. Thus, although our infection model may be limited in the context of organisms causing liver injury and sepsis, we argue that a similar mechanism could account for sepsis caused by other pathogens that induce IFN-I responses, oxidative stress, and metabolic reprogramming of the target cells.

In conclusion, our model (Fig. 10) highlights the role of IFNAR and paracrine IFNβ in the pathogenesis of *Ehrlichia*-induced liver injury and sepsis by mechanisms that involve caspase-11-mediated HMGB1 cytosolic translocation and extracellular secretion, which are linked to induction of autophagy, host cell death, and liver injury. Understanding the role of hepatic IFN-I responses during infection with LPS-negative *Ehrlichia* IOE will greatly enhance our knowledge of the mechanisms of liver dysfunction in patients with HME. Similar to other disease models,[43,44] targeting HMGB1 and the IFN-I pathway may provide a novel approach for treatment of *Ehrlichia*-induced liver injury and sepsis.

REFERENCES

1) Prossomariti A, Sokol H, Ricciardiello L. Nucleotide-binding domain leucine-rich repeat containing proteins and intestinal microbiota: pivotal players in colitis and colitis-associated cancer development. Front Immunol 2018;9:1039.
2) Santoni G, Cardinali C, Morelli MB, Santoni M, Nabissi M, Amantini C. Danger- and pathogen-associated molecular patterns recognition by pattern-recognition receptors and ion channels of the transient receptor potential family triggers the inflammasome activation in immune cells and sensory neurons. J Neuroinflammation 2015;12:21.
3) Compan V, Martin-Sanchez F, Baroja-Mazo A, Lopez-Castejon G, Gomez AI, Verkhratsky A, et al. Apoptosis-associated speck-like protein containing a CARD forms specks but does not activate caspase-1 in the absence of NLRP3 during macrophage swelling. J Immunol 2015;194:1261-1273.
4) Latz E, Xiao TS, Stutz A. Activation and regulation of the inflammasomes. Nat Rev Immunol 2013;13:397-411.
5) Chen R, Zeng L, Zhu S, Liu J, Zeh HJ, Kroemer G, et al. cAMP metabolism controls caspase-11 inflammasome activation and pyroptosis in sepsis. Sci Adv 2019;5:eaav5562.
6) Vande Walle L, Lamkanfi M. Pyroptosis. Curr Biol 2016;26: R568-R572.
7) Barry R, John SW, Liccardi G, Tenev T, Jaco I, Chen CH, et al. SUMO-mediated regulation of NLRP3 modulates inflammasome activity. Nat Commun 2018;9:3001.
8) Yin H, Yang X, Gu W, Liu Y, Li X, Huang X, et al. HMGB1-mediated autophagy attenuates gemcitabine-induced apoptosis in bladder cancer cells involving JNK and ERK activation. Oncotarget 2017;8:71642-71656.
9) Ismail N, Bloch KC, McBride JW. Human ehrlichiosis and anaplasmosis. Clin Lab Med 2010;30:261-292.
10) **Kader M**, **Alaoui-El-Azher M**, Vorhauer J, Kode BB, Wells JZ, Stolz D, et al. MyD88-dependent inflammasome activation and autophagy inhibition contributes to Ehrlichia-induced liver injury and toxic shock. PLoS Pathog 2017;13:e1006644.
11) Ismail N, Soong L, McBride JW, Valbuena G, Olano JP, Feng HM, et al. Overproduction of TNF-alpha by CD8+ type 1 cells and down-regulation of IFN-gamma production by CD4+ Th1 cells contribute to toxic shock-like syndrome in an animal model of fatal monocytotropic ehrlichiosis. J Immunol 2004;172:1786-1800.
12) Lin M, Rikihisa Y. Ehrlichia chaffeensis and Anaplasma phagocytophilum lack genes for lipid A biosynthesis and incorporate cholesterol for their survival. Infect Immun 2003;71:5324-5331.
13) **Huang H**, **Lin M**, Wang X, Kikuchi T, Mottaz H, Norbeck A, et al. Proteomic analysis of and immune responses to Ehrlichia chaffeensis lipoproteins. Infect Immun 2008;76:3405-3414.
14) Yang Q, Stevenson HL, Scott MJ, Ismail N. Type I interferon contributes to noncanonical inflammasome activation, mediates immunopathology, and impairs protective immunity during fatal infection with lipopolysaccharide-negative ehrlichiae. Am J Pathol 2015;185:446-461.
15) Ghose P, Ali AQ, Fang R, Forbes D, Ballard B, Ismail N. The interaction between IL-18 and IL-18 receptor limits the magnitude of protective immunity and enhances pathogenic responses following infection with intracellular bacteria. J Immunol 2011;187:1333-1346.
16) Niu H, Xiong Q, Yamamoto A, Hayashi-Nishino M, Rikihisa Y. Autophagosomes induced by a bacterial Beclin 1 binding protein facilitate obligatory intracellular infection. Proc Natl Acad Sci U S A 2012;109:20800-20807.
17) Lina TT, Luo T, Velayutham TS, Das S, McBride JW. Ehrlichia activation of Wnt-PI3K-mTOR signaling inhibits autolysosome generation and autophagic destruction by the mononuclear phagocyte. Infect Immun 2017;85:e00690-17.
18) Rikihisa Y. Role and function of the type IV secretion system in Anaplasma and Ehrlichia species. Curr Top Microbiol Immunol 2017;413:297-321.
19) Zhang Y, Thai V, McCabe A, Jones M, MacNamara KC. Type I interferons promote severe disease in a mouse model of lethal ehrlichiosis. Infect Immun 2014;82:1698-1709.
20) Crispe IN. Hepatocytes as immunological agents. J Immunol 2016;196:17-21.
21) Robinson MW, Harmon C, O'Farrelly C. Liver immunology and its role in inflammation and homeostasis. Cell Mol Immunol 2016;13:267-276.
22) Gaul S, Leszczynska A, Alegre F, Kaufmann B, Johnson CD, Adams LA, et al. Hepatocyte pyroptosis and release of inflammasome particles induce stellate cell activation and liver fibrosis. J Hepatol 2020;4:S0168-8278(20)30522-5.
23) Rikihisa Y, Kawahara M, Wen B, Kociba G, Fuerst P, Kawamori F, et al. Western immunoblot analysis of Haemobartonella muris and comparison of 16S rRNA gene sequences of H. muris, H. felis, and Eperythrozoon suis. J Clin Microbiol 1997;35:823-829.
24) Stevenson HL, Jordan JM, Peerwani Z, Wang HQ, Walker DH, Ismail N. An intradermal environment promotes a protective type-1 response against lethal systemic monocytotropic ehrlichial infection. Infect Immun 2006;74:4856-4864.
25) Tominello TR, Oliveira ERA, Hussain SS, Elfert A, Wells J, Golden B, et al. Emerging roles of autophagy and inflammasome in ehrlichiosis. Front Immunol 2019;10:1011.
26) Eshleman EM, Lenz LL. Type I interferons in bacterial infections: taming of myeloid cells and possible implications for autoimmunity. Front Immunol 2014;5:431.

27) Smith JNP, Zhang Y, Li JJ, McCabe A, Jo HJ, Maloney J, et al. Type I IFNs drive hematopoietic stem and progenitor cell collapse via impaired proliferation and increased RIPK1-dependent cell death during shock-like ehrlichial infection. PLoS Pathog 2018;14:e1007234.
28) Broz P, Monack DM. Noncanonical inflammasomes: caspase-11 activation and effector mechanisms. PLoS Pathog 2013;9:e1003144.
29) Rao Y, Wan Q, Su H, Xiao X, Liao Z, Ji J, et al. ROS-induced HSP70 promotes cytoplasmic translocation of high-mobility group box 1b and stimulates antiviral autophagy in grass carp kidney cells. J Biol Chem 2018;293:17387-17401.
30) Zhu X, Messer JS, Wang Y, Lin F, Cham CM, Chang J, et al. Cytosolic HMGB1 controls the cellular autophagy/apoptosis checkpoint during inflammation. J Clin Invest 2015;125:1098-1110.
31) Hu W, Chan H, Lu L, Wong KT, Wong SH, Li MX, et al. Autophagy in intracellular bacterial infection. Semin Cell Dev Biol 2020;101:41-50.
32) Khandia R, Dadar M, Munjal A, Dhama K, Karthik K, Tiwari R, et al. A comprehensive review of autophagy and its various roles in infectious, non-infectious, and lifestyle diseases: current knowledge and prospects for disease prevention, novel drug design, and therapy. Cells 2019;8:674.
33) Rikihisa Y. Subversion of RAB5-regulated autophagy by the intracellular pathogen *Ehrlichia chaffeensis*. Small GTPases 2019;10:343-349.
34) McNab F, Mayer-Barber K, Sher A, Wack A, O'Garra A. Type I interferons in infectious disease. Nat Rev Immunol 2015;15:87-103.
35) Wang JY, Zhu B, Patterson LL, Rogan MR, Kibler CE, McBride JW. Ehrlichia chaffeensis TRP120-mediated ubiquitination and proteasomal degradation of tumor suppressor FBW7 increases oncoprotein stability and promotes infection. PLoS Pathog 2020;16:e1008541.
36) Luo T, Mitra S, McBride JW. Ehrlichia chaffeensis TRP75 Interacts with host cell targets involved in homeostasis, cytoskeleton organization, and apoptosis regulation to promote infection. mSphere. 2018;3:e00147-18.
37) De Filippo K, Henderson RB, Laschinger M, Hogg N. Neutrophil chemokines KC and macrophage-inflammatory protein-2 are newly synthesized by tissue macrophages using distinct TLR signaling pathways. J Immunol 2008;180:4308-4315.
38) Yang Q, Ghose P, Ismail N. Neutrophils mediate immunopathology and negatively regulate protective immune responses during fatal bacterial infection-induced toxic shock. Infect Immun 2013;81:1751-1763.
39) Deng M, Tang Y, Li W, Wang X, Zhang R, Zhang X, et al. The endotoxin delivery protein HMGB1 mediates caspase-11-dependent lethality in sepsis. Immunity 2018;49:740-753.e7.
40) Yan Q, Lin M, Huang W, Teymournejad O, Johnson JM, Hays FA, et al. *Ehrlichia* type IV secretion system effector Etf-2 binds to active RAB5 and delays endosome maturation. Proc Natl Acad Sci U S A 2018;115:E8977-E8986.
41) Davis BK, Wen H, Ting JP. The inflammasome NLRs in immunity, inflammation, and associated diseases. Annu Rev Immunol 2011;29:707-735.
42) Jo EK, Kim JK, Shin DM, Sasakawa C. Molecular mechanisms regulating NLRP3 inflammasome activation. Cell Mol Immunol 2016;13:148-159.
43) Lu B, Wang C, Wang M, Li W, Chen F, Tracey KJ, et al. Molecular mechanism and therapeutic modulation of high mobility group box 1 release and action: an updated review. Expert Rev Clin Immunol 2014;10:713-727.
44) Wang W, Wu L, Li J, Ji J, Chen K, Yu Q, et al. Alleviation of hepatic ischemia reperfusion injury by oleanolic acid pretreating via reducing HMGB1 release and inhibiting apoptosis and autophagy. Mediators Inflamm 2019;2019:3240713.

Author names in bold designate shared co-first authorship.

Supporting Information

Additional Supporting Information may be found at onlinelibrary.wiley.com/doi/10.1002/hep4.1608/suppinfo.